JOURNAL OF GEOPHYSICAL RESEARCH, VOL. 104, NO. E5, PAGES 11,875–11,882, MAY 25, 1999

The topography of Tycho Crater

Jean-Luc Margot[1] and Donald B. Campbell
Department of Astronomy, Cornell University, Ithaca, New York

Raymond F. Jurgens and Martin A. Slade
Jet Propulsion Laboratory, Pasadena, California

Abstract. Three-dimensional mapping of the Moon can be accomplished with an Earth-based radar interferometer. Elevation data and radar imagery obtained with this technique are presented for the Tycho Crater area, with a spatial resolution of 200 m and a height resolution of 30 m. The radar maps are displayed in standard cartographic projections with appropriate corrections for elevation-induced geometric distortions. The digital elevation model allows detailed morphometry of the 85 km diameter crater: the floor of Tycho lies 3970 m below a 1738 km radius sphere, and the crater's central peak rises 2400 m above the floor. The average rim crest elevation is 730 m above the 1738 km datum, giving a mean rim to floor depth of 4700 m. The floor has two distinct units with the western section being higher in elevation by ~200 m. This dichotomy is consistent with an asymmetry in the crater shape which reveals that maximum wall slumping occurred in the western and southwestern regions of the crater. Comparison of the radar-derived topography with 87 altimetry points from the Clementine lidar experiment shows rms deviations of ~90 m after a 0.11° latitude correction to the location of all the Clementine altimetry points.

1. Introduction

Earth-based radar interferometry improves our characterization of lunar topography in two important ways: It can provide measurements of the largely unknown topography in the polar regions, and it offers altimetry data with dense (~100 m) horizontal sampling. Elevation data near the lunar poles may refine global models of lunar topography [*Smith et al.*, 1997], which currently rely on interpolation over the polar areas. Digital elevation models of high-latitude regions should also contribute to lunar ice investigations by facilitating the determination of permanently shadowed areas. Other fields of research, such as cratering studies, may benefit from height measurements at the fine horizontal spacings afforded by the radar. Detailed topography may also provide insights about lunar internal structure if used in combination with high-resolution gravity models.

A sequence of Earth-based radar observations was designed to map the polar regions and a few other areas of interest at high spatial (~100 m) and height (~50 m) resolutions. This paper presents elevation maps and rectified radar imagery for a region of the Moon surrounding Tycho Crater (43°S, 349°E). A careful comparison of the radar-derived topography with Clementine altimetry points reveals a very good agreement between the two techniques. Our digital elevation model of the Tycho region is used to measure a few key parameters of the crater's shape and to examine a dichotomy in crater floor units.

Apart from their intrinsic interest, elevation maps enhance the accuracy and usefulness of the radar imagery. Traditionally, radar products cannot be projected onto a two-dimensional surface without introducing geometric distortions such as foreshortening and layover. These distortions can be avoided provided that the topography of the terrain is known [*Curlander and McDonough*, 1991]. In this study, we have used our elevation measurements to provide cartographic projections of the radar imagery which are free of such distortions.

Radar maps of the nearside of the Moon have been obtained at wavelengths of 3.8 cm by *Zisk et al.* [1974] and at 70 cm by *Thompson* [1987], with resolutions of 1-2 km and 3-5 km, respectively. Radar observations of Tycho Crater at those wavelengths were performed by *Pettengill and Thompson* [1968]. By implementing focusing techniques reminiscent of synthetic aperture

[1]Now at National Astronomy and Ionosphere Center, Arecibo, Puerto Rico

Paper number 1998JE900047.
0148-0227/99/1998JE900047$09.00

radar (SAR), *Stacy* [1993] obtained lunar imagery at resolutions of ~100 m and less. The results presented by those investigators include backscatter maps but no topographic measurements.

Detailed topographic maps of the lunar surface can be acquired with an Earth-based radar interferometer in a manner similar to that of interferometric SAR topographic mapping of the Earth. The measurements rely on range differences between points on the lunar surface and two receivers located on Earth. A description of radar-based techniques for measuring lunar topography, including radar interferometry, appeared in the work of *Shapiro et al.* [1972]. *Zisk* [1972b] obtained measurements of lunar topography with the Haystack-Westford radar systems and published results for the Alphonsus-Arzachel region [*Zisk*, 1972a] and the Crisium area [*Zisk*, 1978]. The spatial resolution in those experiments was 1-2 km, and the elevation accuracy was of the order of 500 m. By using the original concept with modern instrumentation and processing techniques, we provide accurate digital elevation models of the Moon with essentially 10 times better resolution. Radar interferometry techniques have also been applied to terrestrial mapping [*Zebker and Goldstein*, 1986] and are used with considerable success for a variety of geophysical applications [*Gens and Van Genderen*, 1996].

Spacecraft measurements of lunar topography include vertical metric photography as well as laser altimetry data acquired during Apollo missions 15, 16, and 17 [*Kaula et al.*, 1974]. These measurements were restricted to within roughly ±30° latitude and had absolute errors of the order of 500 m. They form the basis of the lunar topographic orthophotomaps (LTOs) [*Kinsler*, 1976]. Additional LTOs for nonequatorial regions were based on Orbiter IV and V stereo photography. More recently, the Clementine spacecraft [*Nozette et al.*, 1994] carried a light detection and ranging (lidar) instrument which was used as an altimeter [*Smith et al.*, 1997]. The lidar returned valid data for latitudes between 79°S and 81°N, with an along track spacing varying between a few kilometers and a few tens of kilometers. The across track spacing was roughly 2.7° longitude, or ~80 km at the equator. Because the instrument was somewhat sensitive to detector noise and to solar background radiation, multiple triggers were recorded for each laser pulse. An iterative filtering procedure selected 72,548 altimetry points for which the radial error is estimated at 130 m [*Smith et al.*, 1997].

Previous measurements of the topography of Tycho Crater consist of ~20 altimetry points acquired during Clementine's fortieth revolution [*Smith et al.*, 1997] and ~100 spot elevations on the Tycho LTO [*NASA*, 1971]. The quoted uncertainties on the LTO range between 400 and 1100 m. Five relative elevations obtained by shadow measurements are shown on a lunar astronautical chart (LAC) [*USAF and NASA*, 1967].

Earth-based radar observations offer three significant advantages over existing data sets: complete coverage at ~200 m spacing or less, improved height resolution (~30 m), and coverage of the polar regions. However, parts of the Moon which are never visible from Earth or which are in radar shadow cannot be measured.

2. Observations and Data Reduction Methods

The data were obtained with the antennas of the Deep Space Network (DSN) at Goldstone, California, with an observing strategy similar to that described by *Shapiro et al.* [1972]. A 70 m parabolic dish was used to transmit a pulsed binary-coded waveform at a wavelength of 3.5 cm. Three 34 m antennas separated by 10–20 km formed the receiving elements, providing three distinct interferometers. Radar echoes from Tycho were recorded over a ~10 min period.

Separate maps of the (complex) radar backscatter were produced from each receiving site using the conventional delay-Doppler technique [*Evans and Hagfors*, 1968]. This imaging process consists of isolating the radar echo power in time delay (i.e., range from the observer) and Doppler frequency (i.e., velocity relative to the observer). Since scattering elements on the surface of the rotating Moon have distinct ranges and velocities relative to the radar, analysis of the radar echoes in time delay and Doppler frequency constrains the position of scattering elements in two dimensions. The third dimension (elevation) was obtained by measuring the interferometric phase, i.e., the phase difference recorded for each delay-Doppler resolution cell by the two receivers forming a given interferometer. Topographic changes can be related to interferometric phase because the location of scattering elements in the fringe pattern of the interferometer is elevation-dependent [*Shapiro et al.*, 1972]. In practice, the phase values corresponding to a reference ellipsoid were calculated from ephemerides and subtracted from the measured interferometric phases. Residual phase deviations were then unwrapped [*Goldstein et al.*, 1988] from their natural $[0, 2\pi]$ interval into a continuous phase function spanning several cycles. The unwrapped phases, which represent heights above the assumed reference surface, were then scaled to yield elevations at each resolution cell. A constant phase offset over the entire map was removed by tying the heights to several existing altimetry points obtained during the Clementine mission [*Smith et al.*, 1997].

Resampling the radar image (and its associated elevation model) to a cartographic projection was accomplished by computing the mapping between delay-Doppler and latitude-longitude from ephemeris data. Care was taken to avoid the introduction of geometric distortions at this stage. Distortions in radar imagery (e.g., foreshortening and layover) occur when attempting to project a three-dimensional surface onto a plane without taking the topography into account. In order to circumvent this problem, we used our elevation data in

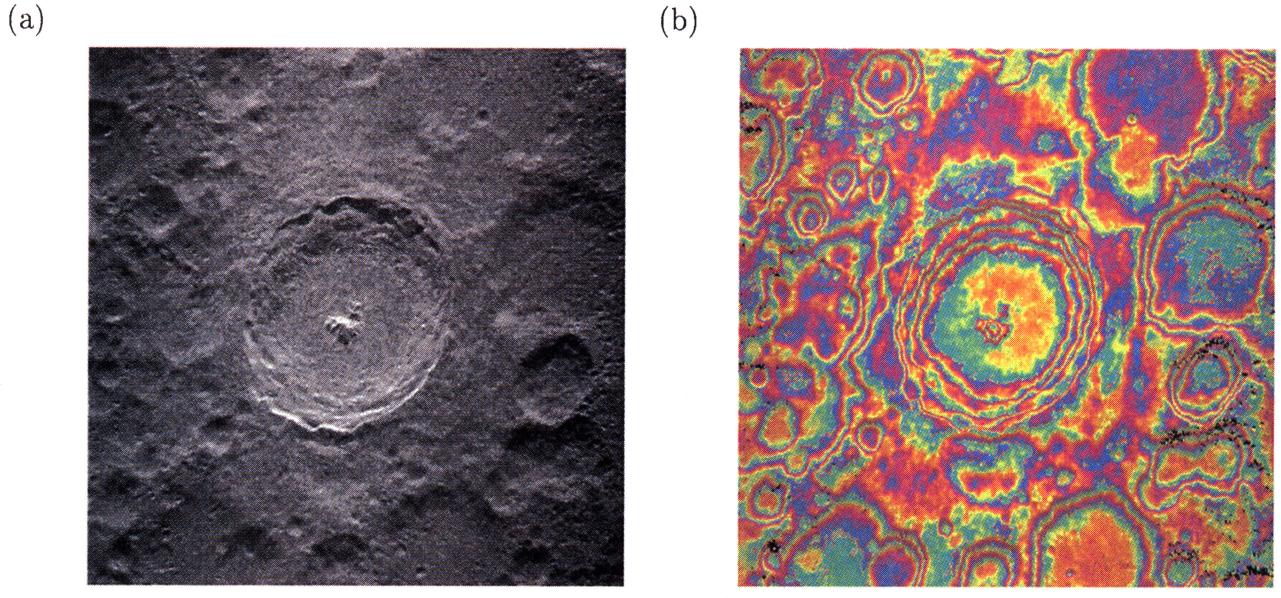

Plate 1. (a) Radar backscatter map of the Tycho region. The image is in delay-Doppler coordinates, with time delay (range from the observer) increasing to the bottom and Doppler frequency increasing to the left. (b) Interferogram corresponding to the same area. The spacing between identical colors represents 360° of phase, or an elevation difference of 1290 m.

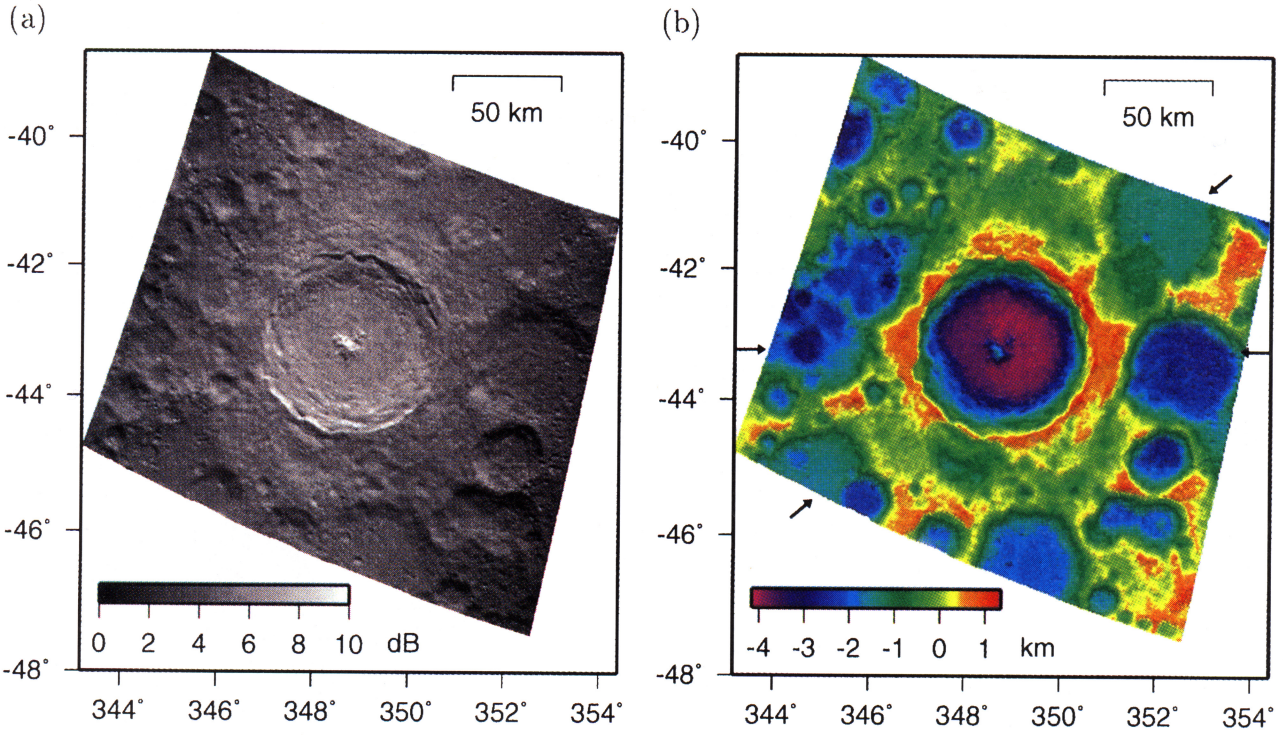

Plate 2. (a) Rectified radar imagery of Tycho Crater shown in a Mercator projection, with east longitude on the horizontal axis. An arbitrary logarithmic scale is used to represent differences in radar backscatter. The radar echo was received in the circular polarization sense opposite to that transmitted. (b) Digital elevation model of the same region. Heights displayed in the elevation map are from -4100 to +1300 m with respect to a 1738 km sphere. The arrows refer to topographic profiles shown in Figure 1.

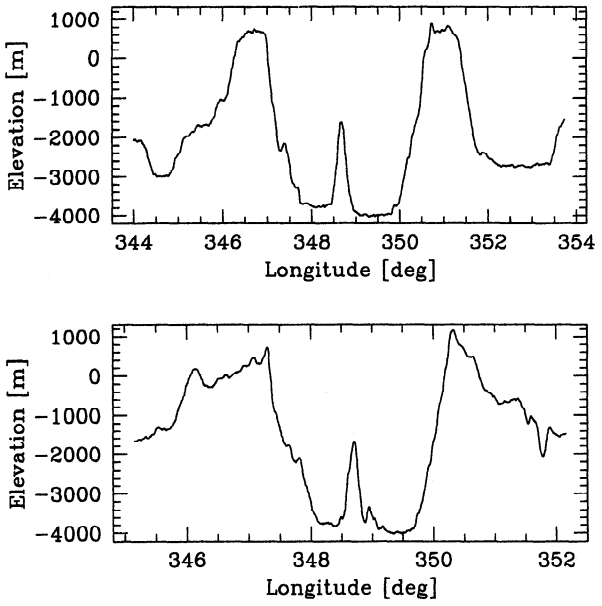

Figure 1. Topographic profiles across Tycho for (top) east-west and (bottom) southwest-northeast. Profile locations are illustrated in Plate 2b.

conjunction with the layover equations [*Curlander and McDonough*, 1991], and we applied the required corrections to each resolution cell.

Radar interferometry concepts, the experiment design, and processing techniques are described in detail elsewhere [*Margot*, 1999].

3. Results

Plate 1a shows a map of radar backscatter for the Tycho region. The image is in delay-Doppler coordinates and covers a 200 x 200 km area. Radar illumination is from the top of the image, as is evidenced by the stronger radar return of the radar-facing inner wall of Tycho.

A map of the interferometric phase for the same area is shown in Plate 1b, which illustrates residual phase deviations obtained after the removal of the phase due to a reference 1738 km sphere. In this interferogram the fringe phase of each resolution element was color coded, and the amplitude of the radar backscatter was used to modulate the brightness of each pixel. Flat areas stand out as they exhibit a uniform phase.

Mercator projections of the radar backscatter and elevation data are displayed in Plates 2a and 2b, respectively. Note that typical distortions present in radar imagery (such as foreshortened slopes and asymmetry in the crater shape) have been effectively removed by the rectification process described in section 2. Correcting geometric distortions shifted the position of elevated features away from the observer, since those features are closer in range than equivalent points at zero elevation are. Similarly, pixels with negative elevations were displaced toward the observer so that they would not masquerade as distant features in the projected image. The largest corrections occurred for the deep floor of Tycho, which was translated by ~3 km compared with its position in the raw radar image.

The rectified image and rectified elevation model were compared to Clementine photomosaic image products in an attempt to validate the mapping procedure as well as the quality of the radar-derived latitude-longitude grid. Match pointing of small features located throughout the scene with Clementine high-resolution imagery revealed that the radar grid seems to be offset by ~0.03° longitude (i.e., ~700 m). Whether the small observed offset is attributable to errors in the Clementine base map or in the radar data is not clear. An error of roughly 0.04 Hz in our calculations of the expected Doppler frequency would produce such a longitudinal shift. Alternatively, it is not inconceivable that the Clementine data exhibit a slight offset. In latitude the registration procedure showed an excellent agreement with Clementine image products, down to the pixel resolution (200 m). The rectified radar products therefore agree perfectly with Clementine imagery in latitude and have a small systematic offset in longitude.

The digital elevation model shown in Plate 2b was obtained by using two antennas separated by 10 km, such that a 360° phase change at the interferometer maps into elevation differences of 1290 m. A separate elevation map (not shown) was constructed independently by using a different combination of receive antennas, with a full phase cycle corresponding to a spacing of 675 m. Error estimates for the elevation data can be obtained by simple proportion of these phase-height relationships. With the signal-to-noise ratio available in this experiment, the theoretical accuracy in interferometric phase measurements [*Vinokur*, 1965] is 10-15°, and the expected height resolutions are therefore of the order of 30 m. We verified that this resolution had indeed been achieved in two different ways. First, we examined heights over presumably flat areas such as crater floors, and we obtained rms deviations of roughly 30 m.

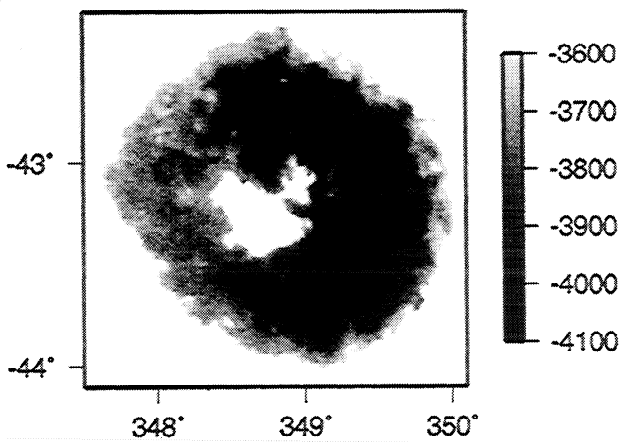

Figure 2. Elevation map of the Tycho floor. Contour levels between -4100 and -3600 m are represented on a gray scale. Note the crater to the northwest of the central peak and the numerous mounds dispersed throughout the floor.

This tends to indicate that the height resolution might be better than 30 m, as a fraction of this value certainly includes real topography. Second, we compared two elevation maps over the entire 40,000 km^2 scene, and we found that the rms deviation between them was 45 m. As the maps were obtained independently of each other, this value again argues for individual height resolutions of the order of 30 m for each map.

One-dimensional profiles across Tycho are shown in Figure 1. The profiles cut across the crater center and central peak in the east-west and southwest-northeast directions, respectively. The peak is 1600 m below the 1738 km datum, roughly 2400 m above the lowest floor level. Note that the west side of the crater floor is ~200 m higher in elevation than the east side, while the west rim is lower than the east rim.

Figure 2 displays crater floor elevations. Whereas most of the terrain lies between elevations of -4000 and -3900 m, a significant fraction of the floor to the west lies near the -3700 contour level. This difference is already apparent on the interferogram in Plate 1b. Although a dichotomy in floor elevations is obvious on both the LAC [*USAF and NASA*, 1967] and LTO [*NASA*, 1971], they were reported as ~600 and ~1000 m, respectively, while our data indicate a ~200 m difference. Excluding the elevated area to the west, the mean floor elevation is -3970 m. The floor diameter measured at the -3700 m contour line is 48 km.

A detailed picture of rim crest elevations as a function of azimuth angle is shown in Figure 3. The rim crest elevation varies between 200 and 1200 m, with a mean value of 730 m. The average rim to floor depth of Tycho is therefore 4700 m. An average rim height with respect to the terrain outside the crater flanks appears to be ~900 m. This number is uncertain owing to the complexity of the terrain surrounding Tycho and the absence of an obvious level surface that can serve as a reference.

4. Discussion

The digital elevation model obtained by radar interferometry offers new opportunities for the study of the crater's morphology. Earlier measurements [*Pike*, 1980] of floor diameter (46 km) and crater depth (4600 m) from shadow data are in good agreement with our values (4700 m and 48 km, respectively). The 2400 m rim height obtained by *Pike* [1980] differs appreciably from the value obtained in this study (~900 m). The discrepancy might be explained by the irregular topography around Tycho and the difficulty in estimating the pre-crater datum. Rim height measurements involving the floors of large adjacent craters as a reference level would overestimate the actual height. Theoretical considerations outlined by *Melosh* [1989] predict a rim height of the order of 1200 m for a crater the size of Tycho. *Pike* [1980] gave an expression for the rim height as a function of crater diameter based on the morphometry of 38 large craters. The expected rim height given by this regression curve is 1400 m.

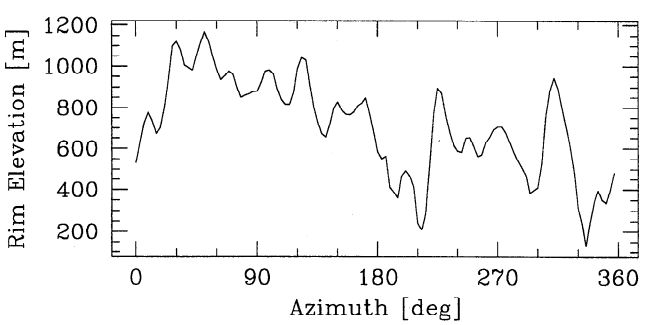

Figure 3. Rim crest elevation of Tycho as a function of azimuth angle. Azimuth is measured from the north, increasing in positive value toward the east.

The dichotomy in floor elevations shown in Figure 2 appears to correlate with two distinct floor units as revealed by Orbiter photography [*Schultz*, 1976]. The high-elevation region to the west of the crater floor corresponds to hummocky terrain while the rest of the floor forms smoother plains. Such differences in floor texture are not unique to Tycho as the floors of Copernicus and Aristarchus also display distinct terrain types [*Schultz*, 1976]. A possible interpretation for the texture and elevation differences lies in differential slumping of the crater wall. Examination of the profiles in Figures 1 and 3 reveals a fundamental asymmetry in the crater shape. Not only are the rim elevations generally low toward the west, but the terraced walls are also wider in the western and southwestern parts of the crater. Maximum wall slumping appears to have occurred in those regions, and the accumulation of debris might have caused higher elevations and rougher terrain type at the bottom of the crater. As discussed by *Schultz and Anderson* [1996], the increased flow debris, wider wall slump zone, and reduced rim height may be related to an oblique impact with a trajectory from the southwest, consistent with ejecta asymmetries.

5. Comparison of Radar Topographic Mapping with Clementine Altimetry

The Clementine lidar [*Smith et al.*, 1997] returned altimetry data over Tycho during its revolution 40. A one-dimensional profile matching this particular Clementine track was extracted from our digital elevation model. This profile, shown in Figure 4, is approximately north-south and cuts across the crater on the east side of the central peak. The rise in elevation near -43° latitude corresponds to the side of a small structure located north of the central peak. The Clementine altimetry points are displayed along the profile. The agreement with the radar data is quite good, except for the datum at -43.52° latitude, which has a height of almost 600 m above the crater floor. Examination of the radar imagery and Clementine optical data shows no sign of a topographic high near this location. In fact, the area appears quite flat, and this particular altimetry datum seems to be in error. Since the lidar instrument onboard

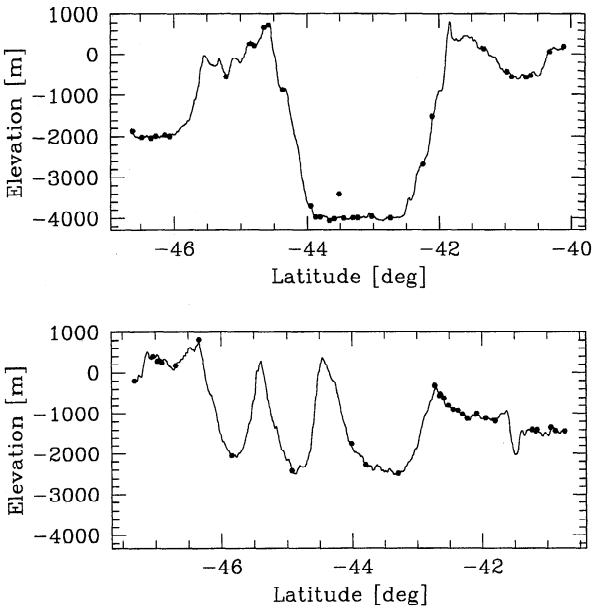

Figure 4. Two topographic profiles which approximate the trajectory of the Clementine spacecraft during its revolutions (top) 40 and (bottom) 39. The Clementine altimetry points are shown as dots superimposed on the radar-derived elevation data. Errors appear larger than they are because the topographic profiles are straight lines while the Clementine points are not exactly aligned. The datum at -43.52° latitude on the top profile appears to be an outlier. Clementine revolutions 39 and 40 yielded the two easternmost tracks shown in Figure 5.

Clementine detected several "hits" for each pulse, the possibility of occasional false triggers and range errors cannot be excluded [*Smith et al.*, 1997]. The profile approximating Clementine track 39 is also shown in Figure 4.

It should be noted that an adjustment to the coordinates of all the Clementine altimetry points was required in order to achieve a good correspondence with the radar data. The amplitude of the correction was found to be +0.11° latitude (~3 km on the surface). A small error in the spacecraft attitude or in the pointing of the lidar might be responsible for the discrepancy. Since the radar-derived coordinates for both the imagery and the elevation model agree fairly well with those of the Clementine photomosaic image products, an explanation involving erroneous coordinates for the radar data seems improbable. The discrepancy in latitude coordinates is obvious when comparing the radar-derived heights with all the lidar measurements available over the scene. There are a total of 87 such Clementine points (approximately one altimetry datum per 500 km^2 area). The rms deviation between the two data sets without the latitude correction is ~300 m, while the deviation after applying the correction is only ~90 m. This is illustrated in Figure 5.

Despite the +0.11° latitude discrepancy, it is remarkable that two independent techniques for measuring elevations are in such agreement over the complex Tycho area. A comparison of the radar data with all

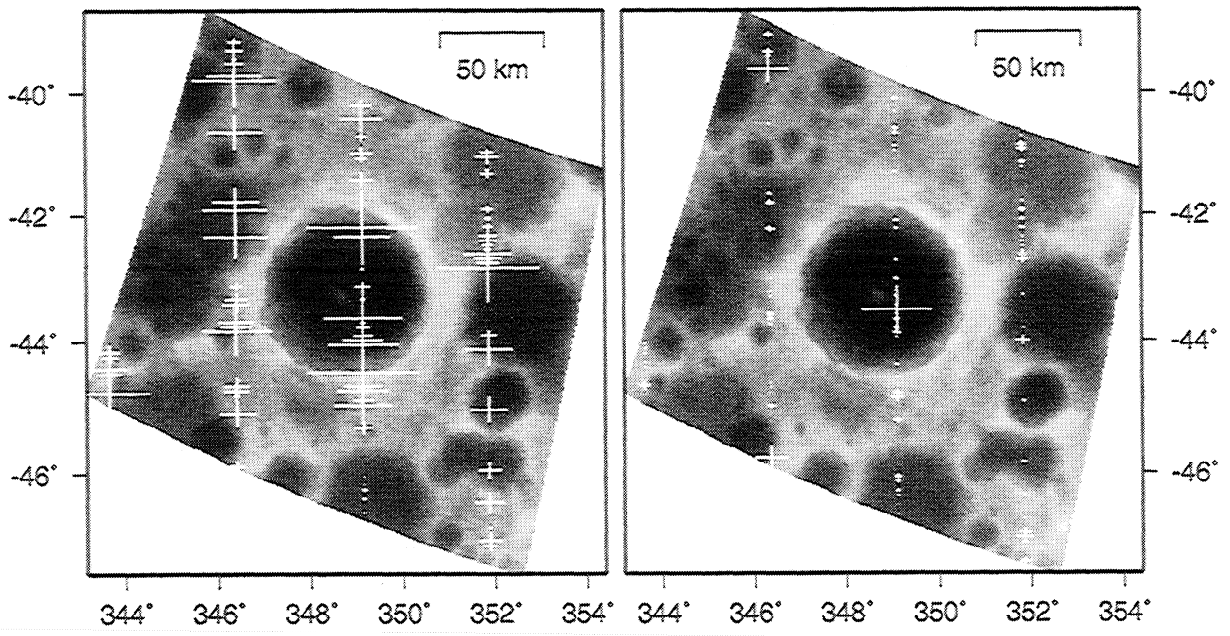

Figure 5. Elevation map of the Tycho area, where the gray scale represents heights from −4100 to +1300 m with respect to a 1738 km radius sphere. Clementine altimetry points collected during revolutions 39–42 (from right to left) are superimposed as white crosses with sizes proportional to the deviation between the radar and Clementine measurements. The left image shows the data uncorrected for latitude shifts (rms deviation ~300 m), and the right image shows the data with a 0.11° correction in the latitude of the Clementine altimetry points (rms deviation ~90 m). The large error bar remaining on the Tycho floor is the outlier discussed in Figure 4.

87 Clementine lidar altimetry points (after the latitude correction) is shown in Figure 6. The rms deviation between the two data sets is 90 m. Given the ~30 m experimental uncertainties in the radar data, this comparison shows that Clementine altimetry data over the Tycho region have radial errors of less than 100 m. The worst-case error is associated with the apparent outlier shown to lie far above the floor of Tycho in Figure 4. Two additional Clementine altimetry points differ from both radar topographic maps by ~300 m in elevation. If all three suspicious altimetry data points are removed from the comparison, the rms deviations between the radar and Clementine elevations are less than 60 m.

6. Conclusions

Earth-based radar interferometry is a powerful technique for the measurement of lunar topography. The technique can produce geometrically rectified maps at spatial resolutions of ~100 m and at height resolutions of ~30 m over hundreds of kilometers. Absolute elevation levels with respect to a reference ellipsoid can be obtained by comparing the heights with existing Clementine altimetry data. For a 200 x 200 km region near Tycho the deviations between the radar-derived elevations and the Clementine altimetry points are ~90 m in a rms sense, after a +0.11° latitude correction to the location of all the altimetry points.

A digital elevation model of Tycho allows detailed morphometry of the crater. The crater depth and height of the central peak are estimated at 4700 and 2400 m, respectively. The rim height is hard to evaluate owing to the complex nature of the terrain surrounding Tycho, and it appears to be of the order of 900 m. A ~200 m elevation difference separates two distinct units on the crater floor. The elevated region can possibly be related to extended wall slumping on the western and southwestern parts of the crater.

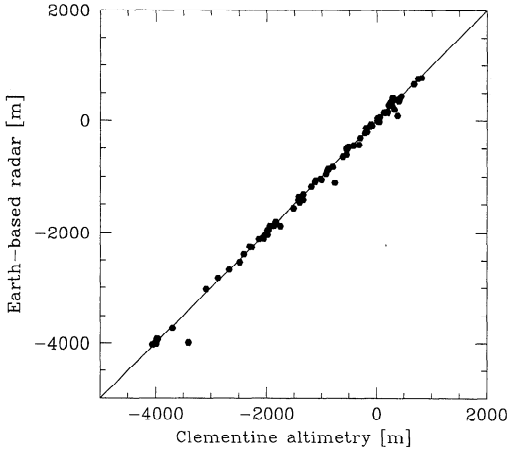

Figure 6. Comparison of all 87 Clementine altimetry points located across the Tycho scene with the radar-derived topography.

Acknowledgments. J.L. Margot and D.B. Campbell were partially supported under NASA grant NAG 5-4220. D.B. Campbell was also partially supported by the National Astronomy and Ionosphere Center, which is operated by Cornell University under a cooperative agreement with the National Science Foundation. Part of this work was supported by the Jet Propulsion Laboratory, operated by the California Institute of Technology under contract with the National Aeronautics and Space Administration. We are grateful to R. Goldstein and H. Zebker for providing their phase unwrapping algorithm; C. Werner, R. Goldstein, and S. Zisk for stimulating discussions about radar interferometry; F. Djuth and J. Elder for assistance with the data acquisition; the Navigation and Ancillary Information Facility (NAIF) group for providing an excellent ephemeris toolkit and associated data files; M. Standish for generating comparison ephemerides; L. Bracamonte for assistance with RF and timing signals, C. Franck for building range-coding equipment; R. Winkler, P. Dendrenos, R. Rose, D. Choate, D. Kelley, J. Garnica, G. Bury, G. Farner, R. Littlefair, C. Snedeker, and C. Franck for assistance with the observations.

References

Curlander, J. C., and R. N. McDonough, *Synthetic Aperture Radar: Systems and Signal Processing.* John Wiley, New York, 1991.

Evans, J. V., and T. Hagfors (Eds.), *Radar Astronomy,* McGraw-Hill, New York, 1968.

Gens, R., and J. L. Van Genderen, Review article: SAR interferometry - issues, techniques, applications, *Int. J. Remote Sens., 17*(10), 1803–1835, 1996.

Goldstein, R. M., H. H. Zebker, and C. L. Werner, Satellite radar interferometry: Two-dimensional phase unwrapping, *Radio Sci., 23*(4), 713–720, 1988.

Kaula, W. M., G. Schubert, R. E. Lingenfelter, W. L. Sjogren, and W. R. Wollenhaupt, Apollo laser altimetry and inferences as to lunar structure, *Lunar Planet. Sci. Conf., 5,* 3049–3058, 1974.

Kinsler, D. C., New lunar cartographic products, *Lunar Planet. Sci. Conf., 7,* i–x, 1976.

Margot, J. L., Lunar topography from Earth-based radar interferometric mapping, Ph.D. thesis, Cornell Univ., Ithaca, N.Y., 1999.

Melosh, H. J., *Impact Cratering: A Geologic Process, Oxford Monogr. Geol. Geophys.,* vol. 11, Oxford Univ. Press, New York 1989.

NASA, Tycho: Orbiter-V-Site 30, lunar topographic photomap, scale 1:250,000, U.S. Army Topogr. Command, 1971.

Nozette, S., et al., The Clementine mission to the Moon: Scientific overview, *Science, 266,* 1835–1839, 1994.

Pettengill, G. H., and T. W. Thompson, A radar study of the lunar crater Tycho at 3.8-cm and 70-cm wavelength, *Icarus, 8,* 457–471, 1968.

Pike, R. J., Geometric interpretation of lunar craters, *U.S. Geol. Survey Prof. Pap., 1046-C,* 1980.

Schultz, P. H., *Moon Morphology: Interpretations Based on Lunar Orbiter Photography.* Univ. of Tex. Press, Austin, Tex., 1976.

Schultz, P. H., and R. R. Anderson, Asymmetry of the Manson impact structure: Evidence for impact angle and direction, in *The Manson Impact Structure, Iowa: Anatomy of an Impact Crater,* edited by C. Koeberl and R. R. Anderson, pp. 397-417, Geol. Soc. of Am., Boulder, Colo., 1996.

Shapiro, I. I., S. H. Zisk, A. E. E. Rogers, M. A. Slade, and T. W. Thompson, Lunar topography: Global determination by radar, *Science*, *178*, 939–948, 1972.

Smith, D. E., M. T. Zuber, G. A. Neumann, and F. G. Lemoine, Topography of the Moon from the Clementine lidar, *J. Geophys. Res.*, *102*(E1), 1591–1611, 1997.

Stacy, N. J. S., High-resolution synthetic aperture radar observations of the Moon, Ph.D. thesis, Cornell Univ., Ithaca, N.Y., 1993.

Thompson, T. W., High-resolution lunar radar map at 70-cm wavelength, *Earth, Moon, Planets*, *37*, 59–70, 1987.

USAF and NASA, Tycho: 112, lunar astronautical chart, scale 1:1,000,000, Aeronaut. Chart and Inf. Cent., 1967.

Vinokur, M., Optimisation dans la recherche d'une sinusoide de période connue en présence de bruit, *Ann. Astrophys.*, *28*(2), 412–445, 1965.

Zebker, H. A., and R. M. Goldstein, Topographic mapping from interferometric synthetic aperture radar observations, *J. Geophys. Res.*, *91*(B5), 4993–4999, 1986.

Zisk, S. H., Lunar topography: First radar-interferometer measurements of the Alphonsus-Ptolemaeus-Arzachel region, *Science*, *178*, 977–980, 1972a.

Zisk, S. H., A new, earth-based radar technique for the measurement of lunar topography, *Moon*, *4*, 296–306, 1972b.

Zisk, S. H., Mare Crisium area topography: A comparison of Earth-based radar and Apollo mapping camera results, *Geochim. Cosmochim. Acta Suppl.*, *9*, 75–80, 1978.

Zisk, S. H., G. H. Pettengill, and G. W. Catuna, High-resolution radar maps of the lunar surface at 3.8-cm wavelength, *Moon*, *10*, 17–50, 1974.

J.-L. Margot, National Astronomy and Ionosphere Center, Arecibo Observatory, HC3 Box 53995, Arecibo, PR 00612, Puerto Rico (margot@naic.edu)

D. B. Campbell, Department of Astronomy, Cornell University, Ithaca, NY 14853. (campbell@astrosun.tn.cornell.edu)

R. F. Jurgens and M. A. Slade, Jet Propulsion Laboratory, Mail Stop 238-420, 4800 Oak Grove Drive, Pasadena, CA 91109. (jurgens@radarsun.jpl.nasa.gov; marty@radarsun.jpl.nasa.gov)

(Received August 5, 1998; revised December 10, 1998; accepted December 14, 1998.)